ChemComm

COMMUNICATION

View Article Online
View Journal | View Issue

Cite this: *Chem. Commun.*, 2024, **60**, 6427

Received 9th May 2024,
Accepted 25th May 2024

DOI: 10.1039/d4cc02252a

rsc.li/chemcomm

Anticancer nano-prodrugs with drug release triggered by intracellular dissolution and hydrogen peroxide response†

Aki Shibata,[a] Yoshitaka Koseki,*[a] Keita Tanita,[a] Showa Kitajima,[a] Kouki Oka,[a] Kiyotaka Maruoka,[a] Ryuju Suzuki,[b] Anh Thi Ngoc Dao[c] and Hitoshi Kasai*[a]

We developed prodrug nanoparticles that release drugs through intracellular dissolution and a cancer-specific hydrogen peroxide response. To reveal the unclear mechanism regarding drug release from nanoparticles by reacting with hydrogen peroxide in cancer cells, this study demonstrates the *in vitro* evaluation of drug release kinetics under conditions simulated in cancer cells.

Various drug delivery systems (**DDSs**) have been reported to selectively release drugs in response to cancer intracellular ROS to reduce side effects.[1] Among the **DDSs**, prodrugs designed to release pharmacologically active drugs following specific chemical transformations within cancer cells have become a key research focus.[2] In recent years, numerous prodrugs that trigger drug release *via* reactive oxygen species (**ROS**), which are present in higher concentrations in tumor tissues than in normal tissues, have been developed.[3,4] **ROS** include $^1O_2$, O^{2-}, $^\bullet OH$, and H_2O_2. In particular, the concentration of H_2O_2 in cancer cells (10–100 μM) is significantly higher than that in normal cells (0.0001–0.7 μM).[5,6] Nevertheless, the selectivity against cancer cells is reduced because **ROS** are also present in blood and normal cells,[7] and prodrug molecules can diffuse throughout the body.[8]

Consequently, research has focused on **ROS**-responsive prodrug nanoparticles to increase their selectivity for cancer cells.[9–13] Prodrug nanoparticles with a controlled particle size of 10–200 nm are known to selectively accumulate in the abnormal vascular space surrounding tumour tissues through the enhanced permeability and retention (**EPR**) effect.[14] Conventional prodrug nanoparticles are fabricated by encapsulating the **ROS**-responsive prodrugs in a nanocarrier,[15,16] and there are concerns about the low drug loading rate and side effects of carrier materials.[17] The burst release from nanoparticles may also exhibit unexpected pharmacological effects.[18] Therefore, to eliminate these concerns in conventional systems, our group has developed carrier-free prodrug nanoparticles, called nano-prodrugs (**NPDs**), which are fabricated from only prodrug molecules.[19–22] These **NPDs** maintain in the particle state until reaching cancer cells and do not release drugs.[20] Additionally, we have reported that the **NPDs** exhibit pharmacological effects after being taken up by cancer cells as intact particles.[22] However, the detailed mechanism by which the **NPDs** release drugs in response to cancer intracellular **ROS** remains unclear.

We aimed to develop **NPDs** that release drugs only after reaching cancer cells by designing prodrugs that are stable against esterases existing abundantly in the body[23,24] and that only react with cancerous **ROS** to release drugs. Specifically, we focused on a prodrug (**CPT-TML**), which combines camptothecin (**CPT**), an anticancer drug, with a trimethyl lock (**TML**) group containing H_2O_2-responsive aryl boronic acid.[25] Herein, to accurately reflect the intracellular drug release mechanism of **NPDs**, we performed *in vitro* assessment and the evaluation of drug release kinetics in the "nanoparticles" or "dissolution" state.

To confirm the drug release kinetics in response to intracellular H_2O_2, we designed two versions of **CPT-TML**: one with aryl boronic acid (**ArB(OH)$_2$**) or aryl (**Ar**) on the protecting group (**PG**) of the **TML** group. In **CPT-TML**, we found that esterases cannot directly cleave sterically hindered esters, while the release of **CPT** through the cyclization reaction of the **TML** group occurs by deprotection of the **PG** and conversion to phenol.[26] **CPT-TML-ArB(OH)$_2$** is expected to release **CPT** *via* the 1,6-elimination of *p*-quinone methide and lactonization of the **TML** group after the conversion of boronic acid to alcohol by H_2O_2. Conversely, **CPT-TML-Ar**, which is insensitive to H_2O_2 and esterases, does not release **CPT** (Scheme 1).

[a] *Institute of Multidisciplinary Research for Advanced Materials, Tohoku University2-1-1 Katahira, Aoba-ku, Sendai-shi, Miyagi-ken 980-8577, Japan. E-mail: koseki@tohoku.ac.jp, kasai@tohoku.ac.jp*
[b] *National Institute of Technology, Sendai College, 48 Nodayama, Medeshima-Shiote, Natori-shi, Miyagi-ken 981-1239, Japan*
[c] *Graduated School of Integrated Science and Technology, Nagasaki University, 1-14 Bunkyo-machi, Nagasaki-shi, Nagasaki-ken 852-8521, Japan*

† Electronic supplementary information (ESI) available. See DOI: https://doi.org/10.1039/d4cc02252a

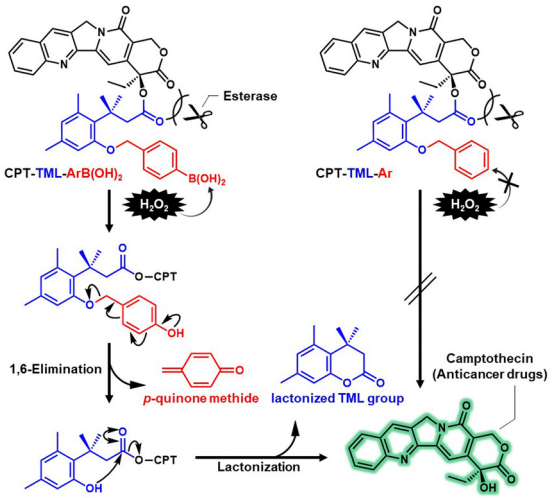

Scheme 1 Proposed **CPT** release mechanism from **CPT-TML**.

CPT-TML-ArB(OH)$_2$ (**11**) was synthesised from 3,5-dimethylphenol (**1**) and methyl 3,3-dimethyl acrylate (**2**) through nine steps shown in Scheme 2, with a total yield of 15% (see the ESI†). **CPT-TML-Ar** (**13**) was obtained *via* the esterification of 3-(2-(benzyloxy)-4,6-dimethylphenyl)-3-methylbutanoic acid (**12**) with **CPT** (Scheme 3). Consequently, **CPT-TML-Ar** (**13**) was synthesised from 3,5-dimethylphenol (**1**) through six steps with a total yield of 8% (for details, please see the ESI†).

The **NPDs** of the synthesized **CPT-TML-ArB(OH)$_2$** and **CPT-TML-Ar** were fabricated using a previously reported reprecipitation method.[27] A solution of **CPT-TML-ArB(OH)$_2$** or **CPT-TML-Ar** in tetrahydrofuran (THF) was injected into vigorously stirred deionized water. Scanning electron microscopy (SEM) images showed that each **NPD** appeared as a spherical nanoparticle,

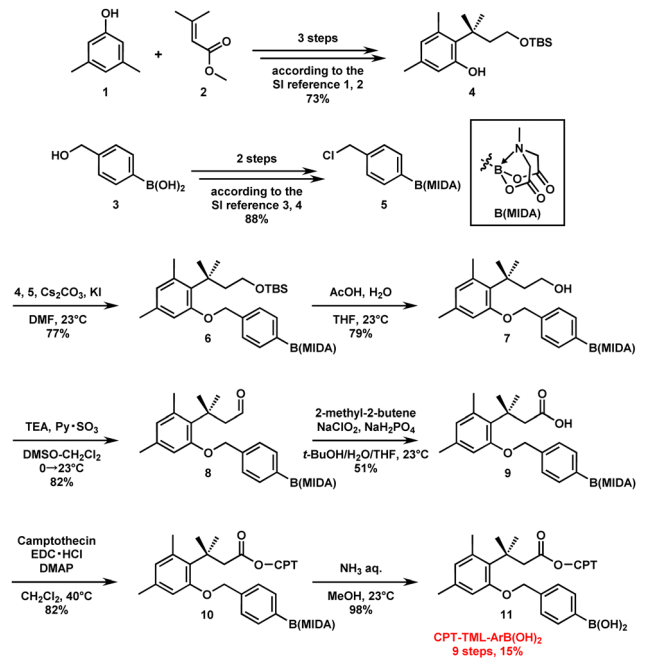

Scheme 2 Synthetic scheme of compound (**11**) (**CPT-TML-ArB(OH)$_2$**).

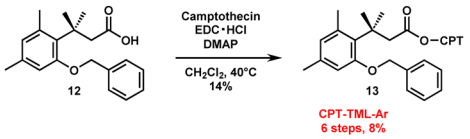

Scheme 3 Synthetic scheme of compound (**13**) (**CPT-TML-Ar**).

with a mean diameter of approximately 100 nm (Fig. 1A and B). In addition, powder X-ray diffraction (PXRD) analysis showed the amorphousness of the fabricated **NPDs** (ESI,† Fig. S1). Although the particle sizes and crystal structures were almost identical, two types of **NPDs** exhibited clear differences in their dispersion stability in water. Dynamic light scattering (DLS) of the hydrodynamic size of the **CPT-TML-ArB(OH)$_2$ NPDs** revealed no significant change even after one month, whereas the **CPT-TML-Ar NPDs** immediately aggregated after reprecipitation (Fig. 1C and D). This may be due to the presence of boronic acid on the surface of the **CPT-TML-ArB(OH)$_2$ NPDs**, which generates electrical repulsive forces,[28] resulting in a higher dispersion stability in water compared to that of the **CPT-TML-Ar NPDs**.

To evaluate the *in vitro* cytostatic activity of the fabricated **NPDs** due to the difference in intracellular H_2O_2 levels, we quantified the H_2O_2 concentration in A549 human lung cancer cells,[22] NHDF-Neo normal dermal fibroblasts, and neonatal cells[29] used to assess the toxicity of nanomedicines. An intracellular H_2O_2 assay was employed with the BIOXYTEC® H_2O_2-560™ Assay Kit based on the intracellular Fenton reaction (ESI†). As a result, the H_2O_2 concentration in A549 cells was presented as 0.13 nmol/10^7 cells. The volume of A549 cells was estimated to be 1670 μm^3 per cell,[30] which would imply a H_2O_2 concentration of approximately 8.1 μM/10^7 cells. The H_2O_2 concentration in A549 cells was about 5-fold higher than that in NHDF-Neo cells (0.028 nmol/10^7 cells) (Fig. 2).

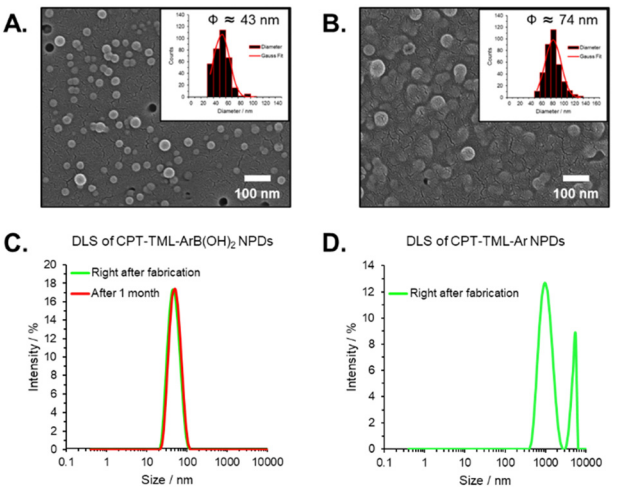

Fig. 1 SEM images of (A) **CPT-TML-ArB(OH)$_2$ NPDs** and (B) **CPT-TML-Ar NPDs**. Inset: Related diameter distribution (Gaussian fitting in red); dispersion stability of (C) **CPT-TML-ArB(OH)$_2$ NPDs** and (D) **CPT-TML-Ar NPDs**; DLS measurement immediately after fabrication (green line) and one month (red line).

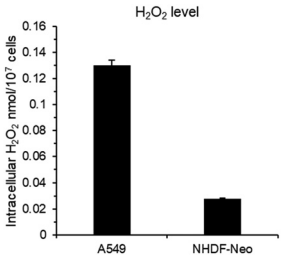

Fig. 2 Intracellular H_2O_2 level of A549 cells and NHDF-Neo cells.

Based on the differences in intracellular H_2O_2 concentrations between cancer and normal cells, we evaluated the *in vitro* cytostatic activities of **CPT-TML-ArB(OH)$_2$ NPDs** and **CPT-TML-Ar NPDs** in A549 and NHDF-Neo cells. **CPT** and lactonized **TML** groups (substituents after the release of **CPT** from **CPT-TML-ArB(OH)$_2$**) were also prepared in accordance with a previous report[26] for comparison of cytostatic activity. **CPT-TML-ArB(OH)$_2$ NPDs**, **CPT-TML-Ar NPDs**, **CPT**, and lactonized **TML** groups in the concentration range of 0.04–10 μM were added to a culture medium comprising A549 cells or NHDF-Neo cells. As shown in Fig. 3A, the **CPT-TML-ArB(OH)$_2$ NPDs** exhibited lower cytostatic activity than **CPT**. Furthermore, the **CPT-TML-Ar NPDs** and lactonized **TML** groups did not exhibit any pharmacological effects. These results indicate that a certain amount of time is required for **CPT** release from **CPT-TML-ArB(OH)$_2$ NPDs** in response to intracellular H_2O_2. Meanwhile, in NHDF-Neo cells, **CPT-TML-ArB(OH)$_2$ NPDs**, **CPT-TML-Ar NPDs**, and lactonized **TML** groups did not reach IC_{50} values of 10 μM except for **CPT** (IC_{50} of **CPT** = 0.98 μM) (Fig. 3B). In particular, the pharmacological effects of the **CPT-TML-ArB(OH)$_2$ NPDs** were high only in cancer cells treated with high H_2O_2 concentrations. To sum up, the **CPT-TML-ArB(OH)$_2$ NPDs** are thought to exhibit pharmacological effects in response to intracellular H_2O_2.

Finally, to verify the prodrug-to-drug conversion, **CPT-TML-ArB(OH)$_2$** and **CPT-TML-Ar** were incubated with 100 μM H_2O_2 (the highest concentration of cancer cells) or esterase from porcine liver in phosphate-buffered saline (PBS) (−), respectively. The release of **CPT-TML-ArB(OH)$_2$**, **CPT-TML-Ar**, **CPT**, and lactonized **TML** was monitored using HPLC-MS/MS analysis. In the case of incubation with 10 units or 100 units of esterase in PBS (−), the **CPT** is seldom released from **CPT-TML-ArB(OH)$_2$ NPDs** and **CPT-TML-Ar NPDs** (ESI,† Fig. S2). Similar

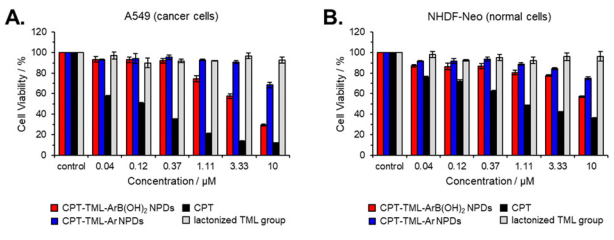

Fig. 3 *In vitro* cytostatic activity of **CPT-TML-ArB(OH)$_2$ NPDs**, **CPT-TML-Ar NPDs**, **CPT**, and the lactonized **TML** group with regard to (A) A549 (cancer cells) and (B) NHDF-Neo (normal cells). These results are indicated as the mean ± standard error (n = 3).

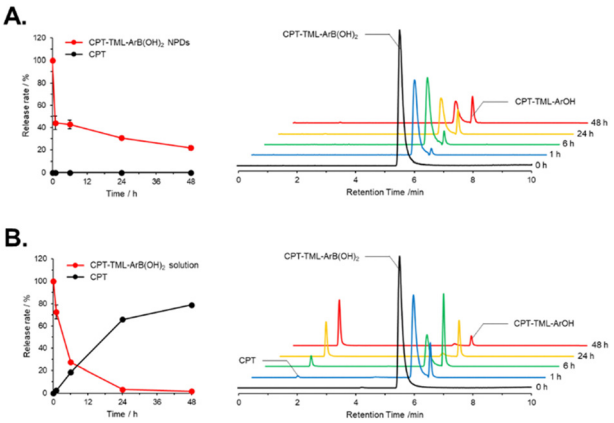

Fig. 4 Release kinetics and HPLC-MS/MS profiles of (A) **CPT-TML-ArB(OH)$_2$ NPDs** in water and (B) **CPT-TML-ArB(OH)$_2$** in DMSO incubated with 100 μM H_2O_2 solution at 37 °C, **CPT-TML-ArOH** is an intermediate in which H_2O_2 converted boronic acid to alcohol. The relative amounts were calculated for each sample based on the concentration of the **CPT-TML-ArB(OH)$_2$** before incubation. These results are indicated as the mean ± standard error (n = 3).

to a previous report,[26] esterase-catalysed hydrolysis of sterically hindered esters in **CPT-TML** was not possible. Moreover, **CPT-TML-Ar** did not release **CPT** after incubation with 100 μM H_2O_2 (ESI,† Fig. S3). When the **CPT-TML-ArB(OH)$_2$ NPDs** were incubated with 100 μM H_2O_2 solution for 48 h, **CPT** was not released, even though an intermediate in which boronic acid was converted to alcohol (**CPT-TML-ArOH**) was gradually detected. In contrast, **CPT-TML-ArB(OH)$_2$** released about 80% **CPT** after 48 h of incubation of the **CPT-TML-ArB(OH)$_2$** DMSO solution in the presence of a 100-μM H_2O_2 solution (Fig. 4B). Simultaneously, a lactonized **TML** group was detected (ESI,† Fig. S5), indicating that **CPT-TML-ArB(OH)$_2$** released **CPT** *via* lactonization of the **TML** group after the conversion of boronic acid to alcohol by intracellular H_2O_2. The results reveal that it is crucial for **CPT-TML-ArB(OH)$_2$ NPDs** to dissolve in cancer cells before responding to intracellular H_2O_2 for the **NPDs** to exhibit pharmacological effects (Scheme 4).

In this study, we synthesized a novel prodrug (**CPT-TML**) consisting of a **TML** group with **ArB(OH)$_2$** on **PG** and **CPT** in a molecular design that releases drugs in response to intracellular H_2O_2. After reprecipitation of **CPT-TML**, we fabricated **NPDs** that were controlled to approximately 100 nm, within the size range relevant to the improvement of tumour accumulation, and stably dispersed for one month in water. The fabricated **CPT-TML NPDs** with pharmacological effects against A549 cancer cells (with a high concentration of H_2O_2) and NHDF-Neo normal cells (with a low concentration of H_2O_2) exhibited clear cytostatic activity in A549 cells, while NHDF-Neo cells maintained over 50% cell viability even with the addition of 10 μM of **CPT-TML NPDs**. In the evaluation of the drug release kinetics of the **CPT-TML** to the H_2O_2 solution, the **CPT-TML NPDs** in water did not release **CPT**, whereas **CPT-TML** dissolved in DMSO could release approximately 80% of **CPT** after 48 h of incubation with a 100-μM H_2O_2 solution. In summary, to effectively release **CPT** from **CPT-TML NPDs**, the **NPDs** must

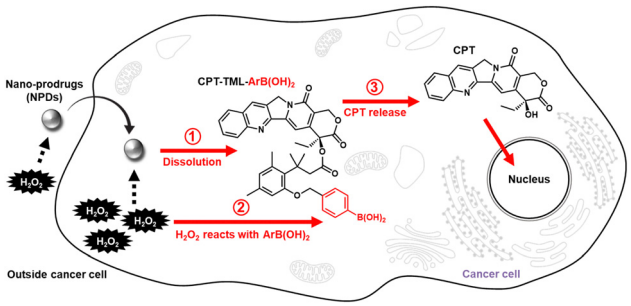

Scheme 4 Schematic representation of the proposed cancer intracellular **CPT** release mechanism from **CPT-TML-ArB(OH)$_2$ NPDs** by H_2O_2 in cancer cells; reactivity of H_2O_2-to-dissolved **CPT-TML-ArB(OH)$_2$** (solid red line) is higher than that of H_2O_2-to-**NPDs** (dotted black line).

dissolve in cancer cells before responding to intracellular H_2O_2. In conclusion, we revealed the process by which **NPDs** react with H_2O_2 in cancer cells to release previously unknown drugs. For the further development of **NPDs** with high cancer selectivity, we must consider both the molecular design that can release drugs through tumour-specific triggers and the solubility of **NPDs** in cancer cells.

This work was supported by JSPS Grants-in-Aid for Scientific Research (No. 22H00328, No. 23K14316), Grant-in-Aid for JSPS Fellows (No. 23KJ0161), JST SPRING (Grant Number JPMJSP2114), the Cooperative Research Program of 'Network Joint Research Center for Materials and Devices', and the Research Program of 'Dynamic Alliance for Open Innovation Bridging Human, Environment and Materials' in 'Network Joint Research Center for Materials and Devices'.

Conflicts of interest

The authors declare that they have no competing financial interest or personal relationships that may have influenced the work reported in this study.

Notes and references

1 C. Robert, C. S. Wilson, A. Venuta, M. Ferrari and C.-D. Arreto, *J. Controlled Release*, 2017, **260**, 226–233.
2 R. Mahato, W. Tai and K. Cheng, *Adv. Drug Delivery Rev.*, 2011, **63**, 659–670.
3 C. J. Prange, X. Hu and L. Tang, *Biomaterials*, 2023, **303**, 122353.
4 B. Chu, H. Deng, T. Niu, Y. Qu and Z. Qian, *Small Methods*, 2023, 2301271.
5 M. Kita, J. Yamamoto, T. Morisaki, C. Komiya, T. Inokuma, L. Miyamoto, K. Tsuchiya, A. Shigenaga and A. Otaka, *Tetrahedron Lett.*, 2015, **56**, 4228–4231.
6 H. Hagen, P. Marzenell, E. Jentzsch, F. Wenz, M. R. Veldwijk and A. Mokhir, *J. Med. Chem.*, 2012, **55**, 924–934.
7 C. M. C. Andrés, J. M. Pérez de la Lastra, C. A. Juan, F. J. Plou and E. Pérez-Lebeña, *Stresses*, 2022, **2**, 256–274.
8 Q. Yao, F. Lin, X. Fan, Y. Wang, Y. Liu, Z. Liu, X. Jiang, P. R. Chen and Y. Gao, *Nat. Commun.*, 2018, **9**, 5032.
9 K.-J. Chen, A. J. Plaunt, F. G. Leifer, J. Y. Kang and D. Cipolla, *Eur. J. Pharm. Biopharm.*, 2021, **165**, 219–243.
10 H. S. El-Sawy, A. M. Al-Abd, T. A. Ahmed, K. M. El-Say and V. P. Torchilin, *ACS Nano*, 2018, **12**, 10636–10664.
11 W. Tao and Z. He, *Asian J. Pharm. Sci.*, 2018, **13**, 101–112.
12 B. Sun, C. Luo, X. Zhang, M. Guo, M. Sun, H. Yu, Q. Chen, W. Yang, M. Wang, S. Zuo, P. Chen, Q. Kan, H. Zhang, Y. Wang, Z. He and J. Sun, *Nat. Commun.*, 2019, **10**, 3211.
13 S. Ma, W. Song, Y. Xu, X. Si, Y. Zhang, Z. Tang and X. Chen, *CCS Chem.*, 2020, **2**, 390–400.
14 S. K. Golombek, J.-N. May, B. Theek, L. Appold, N. Drude, F. Kiessling and T. Lammers, *Adv. Drug Delivery Rev.*, 2018, **130**, 17–38.
15 N. Lu, L. Xi, Z. Zha, Y. Wang, X. Han and Z. Ge, *Biomater. Sci.*, 2021, **9**, 4613–4629.
16 H. Yi, W. Lu, F. Liu, G. Zhang, F. Xie, W. Liu, L. Wang, W. Zhou and Z. Cheng, *J. Nanobiotechnol.*, 2021, **19**, 134.
17 A. Xie, S. Hanif, J. Ouyang, Z. Tang, N. Kong, N. Y. Kim, B. Qi, D. Patel, B. Shi and W. Tao, *EBioMedicine*, 2020, **56**, 102821.
18 J. Yoo and Y.-Y. Won, *ACS Biomater. Sci. Eng.*, 2020, **6**, 6053–6062.
19 Y. Ikuta, S. Aoyagi, Y. Tanaka, K. Sato, S. Inada, Y. Koseki, T. Onodera, H. Oikawa and H. Kasai, *Sci. Rep.*, 2017, **7**, 44229.
20 Y. Koseki, Y. Ikuta, L. Cong, M. Takano-Kasuya, H. Tada, M. Watanabe, K. Gonda, T. Ishida, N. Ohuchi, K. Tanita, F. Taemaitree, A. T. N. Dao, T. Onodera, H. Oikawa and H. Kasai, *Bull. Chem. Soc. Jpn.*, 2019, **92**, 1305–1313.
21 K. Tanita, M. Iijima, Y. Koseki, K. Sato, T. Nakazawa and H. Kasai, *Mol. Cryst. Liq. Cryst.*, 2023, **762**, 81–87.
22 F. Taemaitree, B. Fortuni, Y. Koseki, E. Fron, S. Rocha, J. Hofkens, H. Uji-i, T. Inose and H. Kasai, *Nanoscale*, 2020, **12**, 16710–16715.
23 Y. Yang, H. Aloysius, D. Inoyama, Y. Chen and L. Hu, *Acta Pharm. Sin. B*, 2011, **1**, 143–159.
24 L. Tian, Y. Yang, L. M. Wysocki, A. C. Arnold, A. Hu, B. Ravichandran, S. M. Sternson, L. L. Looger and L. D. Lavis, *Proc. Natl. Acad. Sci. U. S. A.*, 2012, **109**, 4756–4761.
25 H. Maslah, C. Skarbek, S. Pethe and R. Labruère, *Eur. J. Med. Chem.*, 2020, **207**, 112670.
26 A. Shibata, Y. Koseki, K. Tanita, R. Suzuki, A. T. N. Dao and H. Kasai, *Tetrahedron Lett.*, 2022, **103**, 153989.
27 H. Kasai, H. S. Nalwa, H. Oikawa, S. Okada, H. Matsuda, N. Minami, A. Kakuta, K. Ono, A. Mukoh and H. Nakanishi, *Jpn. J. Appl. Phys.*, 1992, **31**, L1132.
28 S. Shrestha, B. Wang and P. Dutta, *Adv. Colloid Interface Sci.*, 2020, **279**, 102162.
29 A. Domiński, T. Konieczny, M. Godzierz, M. Musioł, H. Janeczek, A. Foryś, M. Domińska, G. Pastuch-Gawołek, T. Piotrowski and P. Kurcok, *Pharmaceutics*, 2022, **14**, 2490.
30 R. Jiang, H. Shen and Y.-J. Piao, *Rom. J. Morphol. Embryol.*, 2010, **51**, 663–667.